OPEN

Clinicopathologic and Genetic Features of Primary T-cell Lymphomas of the Central Nervous System

An Analysis of 11 Cases Using Targeted Gene Sequencing

Jeemin Yim, MD, Jiwon Koh, MD, PhD,*† Sehui Kim, MD,*‡ Seung Geun Song, MD,* Jeong Mo Bae, MD, PhD,*† Hongseok Yun, PhD,† Ji-Youn Sung, MD, PhD,§ Tae Min Kim, MD, PhD,‖¶ Sung-Hye Park, MD, PhD,* and Yoon Kyung Jeon, MD, PhD*¶*

Abstract: Primary central nervous system lymphoma (PCNSL) of peripheral T-cell lineage (T-PCNSL) is rare, and its genetic and clinicopathologic features remain unclear. Here, we present 11 cases of T-PCNSL in immunocompetent individuals from a single institute, focusing on their genetic alterations. Seven cases were subject to targeted panel sequencing covering 120 lymphoma-related genes. Nine of the eleven cases were classified as peripheral T-cell lymphoma, not otherwise specified (PTCL-NOS), of which one was of γδT-cell lineage. There was one case of anaplastic lymphoma kinase-positive anaplastic large cell lymphoma and another of extranodal natural killer (NK)/T-cell lymphoma (ENKTL) of αβT-cell lineage. The male to female ratio was 7 : 4 and the age ranged from 3 to 75 years (median, 61 y). Most patients presented with neurological deficits (n = 10) and showed multifocal lesions (n = 9) and deep brain structure involvement (n = 9). Tumor cells were mostly small-to-medium, and T-cell monoclonality was detected in all nine evaluated cases. PTCL-NOS was CD4-positive (n = 4), CD8-positive (n = 3), mixed CD4-positive and CD8-positive (n = 1), or CD4/CD8-double-negative (n = 1, γδT-cell type). Cytotoxic molecule expression was observed in 4 (67%) of the 6 evaluated cases. Pathogenic alterations were found in 4 patients: one PTCL-NOS case had a frameshift mutation in *KMT2C*, another PTCL-NOS case harbored a truncating mutation in *TET2*, and another (γδT-cell-PTCL-NOS) harbored *NRAS* G12S and *JAK3* M511I mutations, and homozygous deletions of *CDKN2A* and *CDKN2B*. The ENKTL (αβT-cell lineage) case harbored mutations in genes *ARID1B*, *FAS*, *TP53*, *BCOR*, *KMT2C*, *POT1*, and *PRDM1*. In conclusion, most of the T-PCNSL were PTCL-NOS, but sporadic cases of other subtypes including γδT-cell lymphoma, anaplastic lymphoma kinase-positive anaplastic large cell lymphoma, and ENKTL were also encountered. Immunophenotypic analysis, clonality test, and targeted gene sequencing along with clinicoradiologic evaluation, may be helpful for establishing the diagnosis of T-PCNSL. Moreover, this study demonstrates genetic alterations with potential diagnostic and therapeutic utility in T-PCNSL.

Key Words: primary CNS lymphoma, primary CNS T-cell lymphoma, targeted gene sequencing, genetic analysis

(*Am J Surg Pathol* 2022;46:486–497)

From the Department of *Pathology; ‖Internal Medicine, Seoul National University Hospital, Seoul National University College of Medicine; †Center for Precision Medicine, Seoul National University Hospital; ‡Department of Pathology, Severance Hospital, Yonsei University College of Medicine; §Department of Pathology, Kyung Hee University School of Medicine; and ¶Cancer Research Institute, Seoul National University, Seoul, Republic of Korea.

Y.K.J. designed and supervised the study; J.Y., S.K., and S.G.S. analyzed the results; J.K., J.M.B., and H.Y. performed bioinformatics analysis; Y.K.J., J.-Y.S., and S.-H.P. performed the pathologic evaluation; T.M.K. reviewed the clinical data; J.Y., J.K., and Y.K.J. wrote the manuscript; all authors read and approved the final manuscript.

This work was supported by the Basic Science Research through the National Research Foundation of Korea (NRF) funded by the Ministry of Education, Science and Technology (MEST) Program (grant No.: NRF-2016R1D1A1B01015964), and the Basic Research Program through the NRF funded by the Ministry of Science and ICT (MSIT) (grant No.: 2020R1A4A1017515), Republic of Korea.

Conflicts of Interest and Source of Funding: The authors have disclosed that they have no significant relationships with, or financial interest in, any commercial companies pertaining to this article.

Correspondence: Yoon Kyung Jeon, MD, PhD, Department of Pathology, Seoul National University College of Medicine, 103 Daehak-ro, Jongno-gu, Seoul 03080, Republic of Korea (e-mail: ykjeon@snu.ac.kr).

Supplemental Digital Content is available for this article. Direct URL citations appear in the printed text and are provided in the HTML and PDF versions of this article on the journal's website, www.ajsp.com.

Primary central nervous system lymphoma (PCNSL) is defined as a lymphoma arising in the central nervous system (including brain, spinal cord, leptomeninges, or eye) without any evidence of systemic manifestation at the time of diagnosis in immunocompetent individuals.[1] PCNSL accounts for 2% to 6% of all primary brain malignancies, and the majority of PCNSL cases are diffuse large B-cell lymphoma (DLBCL).[1] PCNSL of peripheral T-cell lineage (T-PCNSL) is very rare and the incidence of T-PCNSL ranged from 2% to 4% of PCNSL in Western countries and 7% to 9% of PCNSL in East Asian countries.[2–6] In the largest multicenter, multination cases series of T-PCNSL (n = 45), the patients ranged in age from 3 to 84 years (median, 60 y) with an Eastern Cooperative Oncology Group performance status of 0 or 1 in

48% of patients. The majority of patients (64%) had cerebral hemisphere involvement and 36% had involvement of deep brain structures.[6] The prognosis of T-PCNSL was comparable to PCNS-DLBCL, with a median disease-specific survival of 25 months and 2-year and 5-year disease-specific survival rates of 51% and 17%, respectively.[6] However, the clinicopathologic characteristics of T-PCNSL have not been well elucidated.

Recently, a case series of 18 T-PCNSLs involving clinical, morphologic, immunophenotypical, and molecular analysis was reported.[7] Those series included 15 cases of peripheral T-cell lymphoma, not otherwise specified (PTCL-NOS), 2 cases of anaplastic lymphoma kinase (ALK)-negative anaplastic large cell lymphoma (ALCL), and 1 case of ALK-positive ALCL. Most of the PTCL-NOS cases (11/15) involved small and/or medium-sized lymphocytes, which might be diagnostically challenging for T-PCNSL. Similar to PCNS-DLBCL, perivascular cuffing was a characteristic and prominent feature in the majority of cases. In their series, the ratio of CD8 to CD4 lineage tumors was 2 : 1, and most cases showed a cytotoxic phenotype. The authors described genetic alterations of T-PCNSL and demonstrated mutations in *DNMT3A*, *KRAS*, *JAK3*, *STAT3*, *STAT5B*, *GNB1*, and *TET2* genes for the first time using targeted next-generation sequencing.[7]

However, the clinicopathologic, and particularly genetic, features of T-PCNSL remain unclear. Thus, the aim of this study was to demonstrate the clinicopathologic features of T-PCNSL and genetic alterations with potential diagnostic and therapeutic utility in T-PCNSL.

MATERIALS AND METHODS

Case Selection

Eleven cases of T-PCNSL were identified from the pathology database of Seoul National University Hospital (SNUH) between 2005 and 2021. The patients' diagnoses were reviewed and classified according to the 4th World Health Organization classification.[1] An experienced hematopathologist (Y.K.J.) and neuropathologist (S.-H.P.) evaluated the pathologic material. Clinical data including tumor location, initial symptoms, performance status, treatment modalities, and outcomes were obtained from medical records by a hemato-oncologist (T.M.K.). To exclude the presence of systemic disease, whole body positron emission tomography/computerized tomography scan was performed in all the patients and the hemato-oncologist (T.M.K.) confirmed the primary central nervous system (CNS) origin of lymphoma in all patients. One patient (case 9) was previously reported as a single case.[8] This study was approved by the Institutional Review Board (IRB) of SNUH (No. H-1807-070-958). Informed consent for participation in the study was waived by the IRB of SNUH.

Immunohistochemistry and In Situ Hybridization for Epstein-Barr Virus-encoded RNA

Immunohistochemical studies were performed for CD2, CD3, CD4, CD5, CD7, CD8, CD10, CD15, CD20, CD30, CD56, Bcl-2, Bcl-6, C-MYC, MUM-1, PD-1, ICOS, ALK, TdT, TCRβF1, TCRγ, granzyme B, pHH3, and Ki-67 on available formalin-fixed paraffin-embedded tissue (FFPE) sections. Information on the antibodies and staining methods are summarized in Supplementary Table S1 (Supplementary Digital Content 2, http://links.lww.com/PAS/B299). Epstein-Barr virus (EBV) in situ hybridization was performed using the Bond Ready-to-Use ISH EBV-encoded RNA (EBER) probe (Leica Biosystems, Newcastle, UK) or INFORM EBER Probe (Ventana Medical Systems, Tucson, AZ), in conjunction with the Bond-Max autostainer (Leica Microsystems) and Ventana Benchmark XT automated system (Ventana Medical Systems), respectively, according to the manufacturer's protocol.

T-cell Clonality Test

T-cell monoclonality was detected using the IdentiClone TCRG Gene Clonality Assay (Invivoscribe Technologies Inc., San Diego, CA) or multiplex-PCR for the T-cell receptor (TCR)γ gene, followed by heteroduplex analysis as previously described.[9]

Targeted Gene Sequencing

We created a customized panel composed of 120 genes important in the pathogenesis of lymphoid neoplasm (Supplementary Table S2, Supplementary Digital Content 3, http://links.lww.com/PAS/B300). At least 50 ng genomic DNA was extracted from each FFPE sample using the Maxwell FFPE Purification Kit (Promega, Madison, WI). Library preparation was performed using the SureSelect XT-HS Target Enrichment System (Agilent Technologies, Santa Clara, CA). Library concentrations were quantified and assessed by the 4200 TapeStation System (Agilent Technologies). Paired-end sequencing was performed on the Illumina NextSeq. 550Dx Platform (Illumina Inc., San Diego, CA).

Sequencing Data Analyses

Sequencing reads were mapped against the reference genome (GRCh37/hg19) using Burrows-Wheeler Aligner (BWA) (version 0.7.17) and GATK Best Practice (version 4.0.2.1). SNVer (version 0.5.3) and LoFreq (version 2.1.2) were used to call single nucleotide variants (SNVs) and small insertions and deletions (INDELs). A CNVkit was used to identify and visualize copy number variations (CNVs). SnpEff (version 4.3) was used for variant annotation. To exclude possible germline variants in the general population, only variants with allele frequency <0.1% in the Genome Aggregation Consortium East Asian database, Korean Reference Genome Database, and Korean Variant Archive were retained for further analyses.

RESULTS

Clinical Features of Patients With T-PCNSL

The clinical features of the 11 patients with T-PCNSL are summarized in Table 1, and the clinicopathologic features of the cases are briefly described in the Supplementary Information (Supplementary Digital Content 1, http://links.lww.com/PAS/B298). The age of the patients ranged from 3 to 75 (median, 61 y), and the male to female ratio was 7 : 4. None of the patients had a history of immune deficiency. Patients visited the hospital with neurological deficits, visual disturbance, headache, and/or dizziness. Most of the patients showed involvement of deep brain structures (ie, periven-

TABLE 1. Clinical Features of the T-PCNSL Cases

No.	Age/Sex	Dx	Initial Sx	KPS	LDH	Location
1	40/M	PTCL-NOS	Neurologic deficit	90	WNL	Temporal
2	69 /F	PTCL-NOS	Neurologic deficit	60	Elev.	Temporal, parietal, occipital
3	69/F	PTCL-NOS	Neurologic deficit	60	Elev.	Both cerebral hemispheres, cerebellum
4	16/M	ALK(+) ALCL	Headache, dizziness, diplopia	90	Elev.	Parieto-occipital
5	68/F	PTCL-NOS	Neurologic deficit	90	Elev.	Frontal
6	62/M	PTCL-NOS	Visual deficit	90	Elev.	Frontal
7	61/M	PTCL-NOS	Visual deficit	90	WNL	Rt periventricular WM, Lt cerebral peduncle
8	26/M	PTCL-NOS	Neurologic deficit	30	WNL	Basal ganglia
9	75/F	PTCL-NOS (γδT-cell)	Neurologic deficit	30	NA	Spine, Lt lateral periventricular WM
10	3/M	PTCL-NOS	Neurologic deficit†	60	Elev.	Thalamus
11	61/M	ENKTL (αβT-cell)	Intermittent headache	90	Elev.	Lt parietotemporal WM, Rt thalamus, midbrain, and pons, Rt frontoparietal subcortical WM

*Viterous fluid involvement.
†Neurological deficit with cough, sore throat, fever.
ALCL indicates anaplastic large cell lymphoma; autoPBSCT, autologous peripheral blood stem cell transplantation; COPADM, cyclophosphamide, vincristine, prednisolone, doxorubicin, and high-dose methotrexate; CRu, unconfirmed complete response; CT Rx, chemotherapy regimen; CT, chemotherapy; Dx, diagnosis; Elev., elevated; ENKTL, extranodal NK/T-cell lymphoma; IMEP, ifosfamide, methotrexate, etoposide, prednisone; KPS, Karnofsky Performance Score; LDH, lactate dehydrogenase; Lt, left; MA, high-dose methotrexate and cytarabine; mCR, metabolic complete response; modified COP, cyclophosphamide, vincristine and prednisone; MVP, high-dose methotrexate, vincristine, and procarbazine; NA, not available; No., case number; Op, operation; OS, overall survival; PD, progressive disease; PFS, progression-free survival; PR, partial response; PTCL-NOS, peripheral T-cell lymphoma, not otherwise specified; RT, radiotherapy; Rt, right; SD, stable disease; Sx, symptoms; Tx, treatment; WNL, within normal limit.

TABLE 2. Morphology, Immunophenotype, TCR Clonality, and Mutational Status of the T-PCNSL Cases

No.	Dx	Cell size	PVL	CD3	CD4/8	CTM	EBV	TCRβF1	TCRγ
1	PTCL-NOS	Small	Present	(+)	CD4	NA	(−)	NA	NA
2	PTCL-NOS	Small/medium	Present	(+)	CD8	(+)	(−)	(+)	NA
3	PTCL-NOS	Small/medium	Present	(+)	CD4	NA	(−)	(+)	NA
4	ALK(+) ALCL	Large/anaplastic	Present	(−)	NA	NA	(−)	NA	NA
5	PTCL-NOS	Small	Present	(+)	CD4	(+)	(−)	(+)	NA
6	PTCL-NOS	Small	Present	(+)	CD4	(−)	(−)	(+)	NA
7	PTCL-NOS	NA	NA	(+)	NA	NA	(−)	NA	NA
8	PTCL-NOS	Small	Present	(+)	Mixed	NA	(−)	(+)	NA
9	PTCL-NOS (γδT-cell)	Medium/large	Absent	(+)	DN*	(+)	(−)	(−)	(+)
10	PTCL-NOS	Small	Absent	(+)	CD8	(−)	(−)	(+)	(−)
11	ENKTL (αβT-cell)	Large	Present	(+)	CD8	(+)	(+)	(+)	NA

*CD8-positive in <10% of tumor cells.
ALCL indicates anaplastic large cell lymphoma; CTM, cytotoxic molecules (granzyme B or TIA-1); DN, double negative; Dx, diagnosis; ENKTL, extranodal NK/T-cell lymphoma; f+, focal positive; GR, gene rearrangement; IHC, immunohistochemistry; NA, not available; No., case number; PTCL-NOS, peripheral T-cell lymphoma, not otherwise specified; PVL, perivascular lymphocytic cuffing.

TABLE 1. *(continued)*

Deep Structure Involvement	Multi-focality	Vitreoretinal/CSF Involvement	Tx detail	Upfront CT Rx	CT/RT Response	Outcome	PFS, m	OS, m
Yes	Yes	No	OP/CT/RT	MA(×6)	CRu	Alive	122.7	122.7
Yes	Yes	Yes	OP/CT	MVP(×2)	NA	Death	6.5	6.5
Yes	Yes	Yes	CT	MVP(×1)	NA	Death	1.1	20.0
Yes	No	NA	CT/RT/ autoPBSCT	COPADM(×2)	NA	Alive	70.4	70.4
No	No	Yes	CT/RT	MVP(×6)	SD→mCR	Alive	57.0	57.0
No	Yes	Yes*	CT/RT	MVP(×6)	CRu	Alive	55.7	55.7
Yes	Yes	No	CT/RT	MVP(×2)	CRu	Death	27.2	31.6
Yes	Yes	No	CR/RT	MVP(×6)	PR	Alive	56.9	56.9
Yes	Yes	No	OP	NA	NA	Death	3.0	3.0
Yes	Yes	NA	CT	Modified COP	NA	Alive	1.3	33.2
Yes	Yes	No	OP/CT	IMEP+Pegaspargase	PD	Alive	0	3.3

TABLE 2. *(continued)*

Other IHC	*TCG* GR	*IGH* GR	Pathogenic Mutations	VUS Mutations
CD30(a few +), TdT(−), CD5(+)	Monoclonal	Polyclonal	NA	NA
NA	Monoclonal	NA	KMT2C p.Arg380fs	None
CD30(−)	Monoclonal	NA	TET2 p.Leu371*	FAS p.Glu272Gly
CD30(+), CD15(−), ALK(+)	NA	NA	None	None
CD30(−), CD56(−)	Monoclonal	Polyclonal	None	KMT2C p.Gly908Cys KMT2C splicing
CD2(+), CD5(−), CD7(f+), TdT(−)	Monoclonal	Polyclonal	NA	NA
NA	NA	NA	NA	NA
CD2(f+), CD5(f+), CD7(f+)	Monoclonal	Polyclonal	NA	NA
CD103(+), CD56(+), CD30(−)	Monoclonal	NA	NRAS p.Gly12Ser JAK3 p.Met511Ile CDKN2A homozygous deletion CDKN2B homozygous deletion	POT1 p.Lys33Glu KMT2C p.Pro335Ser SMARCA2 p.Gln230_Gln231delinsPro BCL2 p.Ser70Leu
ALK(−), TdT(−)	Monoclonal	NA	None	KMT2C p.Gly908Cys
CD56(+), CD30(−), PD-1(−), ICOS(−)	Monoclonal	NA	ARID1B p.Ser425* BCOR p.Ser158fs FAS splicing TP53 p.Cys135Phe TP53 p.Ala161Val TP53 p.Arg175His KMT2C heterozygous deletion POT1 heterozygous deletion PRDM1 heterozygous deletion	EGR2 p.Pro169Leu NFRKB p.Val786Ile TET2 p.Asn639Tyr BRAF heterozygous deletion EZH2 heterozygous deletion FYN heterozygous deletion GATA3 heterozygous deletion IDH2 heterozygous deletion JAK3 copy number gain MEF2B copy number gain MYD88 copy number gain NOTCH2 copy number gain NFRKB copy number gain PLCG1 copy number gain RELA copy number gain RHOA copy number gain UBR5 copy number gain

tricular regions, basal ganglia, brain stem, and/or cerebellum) (9/11, 81.8%) and multifocal sites (9/11, 81.8%) on initial brain magnetic resonance imaging. The major locations of the lesions included the brain cerebral hemispheres, deeper brain sites, and spine. Cerebrospinal or vitreoretinal involvement was observed in 4 (44.4%) of the 9 patients, including 1 patient (case 6) with vitreoretinal involvement. The majority of patients received high-dose methotrexate in combination with vincristine and procarbazine (n = 6); the others received high-dose methotrexate and cytarabine (n = 1), cyclophosphamide, vincristine, prednisone, doxorubicin, and high-dose methotrexate (n = 1), cyclophosphamide, vincristine, and prednisone (n = 1), or ifosfamide, methotrexate, etoposide, and prednisone (n = 1) as the initial chemotherapy, followed by radiotherapy (n = 6). Two patients (cases 2 and 9) died of disease within 1 year of diagnosis, 1 patient (case 3) after 20 months of diagnosis, and another (case 7) after 31.6 months of diagnosis. One patient (case 10) was referred to hospice care. The median progression-free survival time was 27.2 months, and the median overall survival time was 33.2 months.

Pathologic Features of T-PCNSLs

Pathologic features of the 11 cases with T-PCNSL are summarized in Table 2. The histologic and immunophenotypical features of the cases are described in the Supplementary Information (Supplementary Digital Content 1, http://links.lww.com/PAS/B298). Representative pathologic images are shown in Figures 1–4 and Supplementary Figures S1–S3 (Supplementary Digital Contents 4–6, http://links.lww.com/PAS/B301, http://links.lww.com/PAS/B302, http://links.lww.com/PAS/B303). Nine of the 11 cases were classified as PTCL-NOS (Figs. 1, 2 and 4; Supplementary Figs. S1–S3, Supplementary Digital Contents 4–6, http://links.lww.com/PAS/B301, http://links.lww.com/PAS/B302, http://links.lww.com/PAS/B303) and 1 patient (M/16 y) was diagnosed with ALK-positive ALCL (Figs. 3A–F). Case 11 (M/61 y) was diagnosed with primary CNS extranodal natural killer (NK)/T-cell lymphoma (ENKTL) of αβT-cell lineage; no other extracranial sites with tumor involvement were found on systemic work-up. Of the nine cases of PTCL-NOS, one (F/75 y) was of γδT-cell origin (Figs. 1J–L), the clinicopathologic features of which were previously reported in detail.[8] Tumor cells were small or small-to-medium in the majority of patients (n = 7) (Figs. 1A–I, 2, and 4; Supplementary Figs. S1–S3, Supplementary Digital Contents 4–6, http://links.lww.com/PAS/B301, http://links.lww.com/PAS/B302, http://links.lww.com/PAS/B303), medium-to-large in the patient with PTCL of γδT-cell origin (Fig. 1J–L), large in the patient with ENKTL (Figs. 3G–L), and large-to-anaplastic in the patient with ALK-positive ALCL (Figs. 3A–F). Perivascular lymphocytic infiltration was observed in the majority of cases (8/10, 80%) with 6 cases showing prominent perivascular infiltration (cases 1 [Supplementary Fig. S1B, Supplemental Digital Content 4, http://links.lww.com/PAS/B301], 3, 5, 6 [Fig. S3A, Supplemental Digital Content 6, http://links.lww.com/PAS/B303], 8 (Fig. 2I), and 11 (Fig. 3H).

Detailed morphologic features of representative cases were as follows: in case 1 (PTCL-NOS), small lymphoid cells with mild atypism were infiltrating perivascular area and parenchyme with strong perivascular lymphocyte cuffing (Supplementary Fig. S1, Supplemental Digital Content 4, http://links.lww.com/PAS/B301). In case 2 (PTCL-NOS), geographic necrosis and focal microscopic hemorrhage were observed. At the interface between necrotic area and brain parenchyme, many small-to-medium-sized atypical lymphoid cell were observed. Atypical lymphoid cells were also diffusely infiltrating adjacent brain parenchyme along with perivascular cuffing and involvement of Virchows Robin spaces (Figs. 1B, C). The lymphoid cells had nuclear atypia with irregular or angulated nuclear contour and coarse chromatin and scanty clear cytoplasm (Figs. 1B, C). In microscopic examination of case 3 (PTCL-NOS), the biopsied tissue was hypercellular and densely infiltrated by small-to-medium-sized atypical lymphoid cells and histiocytes (Fig. 2B). Perivascular lymphocytic cuffing was frequently observed and the lymphoid cells showed nuclear atypia with irregular or angulated nuclear contour and scanty clear cytoplasm. In case 9 (PTCL of γδT-cell origin), removed spinal tumor was hypercellular and composed of diffuse and dense infiltration of atypical monomorphic lymphoid cells (Figs. 1J–L). The atypical lymphoid cells were medium-to-large in size and had round nuclei, condense or finely dispersed chromatin, small inconspicuous nucleoli, and pale-to-eosinophilic moderate amount of cytoplasm (Figs. 1J–L). In the patient with ALK-positive ALCL (case 4), microscopic examination revealed diffuse infiltration of large atypical cells with an anaplastic morphology admixed with small lymphocytes, histiocytes, and reactive astrocytes (Figs. 3B–F). CD30 immunostaining highlighted occasional cohesive arrangement of lymphoma cells along with perivascular cuffing (Fig. 3E). Hallmark cells having large eccentric kidney-shaped nuclei and plump cytoplasm were frequently observed (Fig. 3C). In the patient with ENKTL of αβT-cell lineage (case 11), microscopic examination revealed large atypical lymphoid cells infiltration predominantly in Virchows Robin spaces and perivascular area along with perineuronal satellitosis (Figs. 3G, H). The atypical lymphoid cells had large atypical nuclei with finely dispersed chromatin, irregular nuclear membrane, occasional nuclear grooves and multiple small distinct nucleoli. Apoptotic cells were easily detected in any high power field.

Among the cases of PTCL-NOS, 4 (4/8, 50%) were predominantly infiltrated by CD4-positive cells, and 3 (3/8, 37.5%) by CD8-positive cells; 1 case (1/8, 12.5%) showed a mixed pattern with both CD4-positive and CD8-positive cell infiltration. The PTCL of γδT-cell origin was CD4/CD8-double-negative and the ENKTL case was CD8-positive. Cytotoxic molecules (granzyme B or TIA-1) were expressed in the majority (4/6, 66.7%) of evaluated cases. EBV in situ was diffusely positive in ENKTL and negative in the other cases. T-cell monoclonality was detected in all 9 evaluated cases.

Genetic Features of T-PCNSLs

A total of 40 mutations in 28 genes were found in 6 patients; no recurrent mutations were observed (Table 2, Fig. 5). *KMT2C* was the most frequently mutated gene (5/7, 71%) with missense, splicing, and frameshift mutations and copy number alterations, followed by *TET2, FAS, POT1*, and

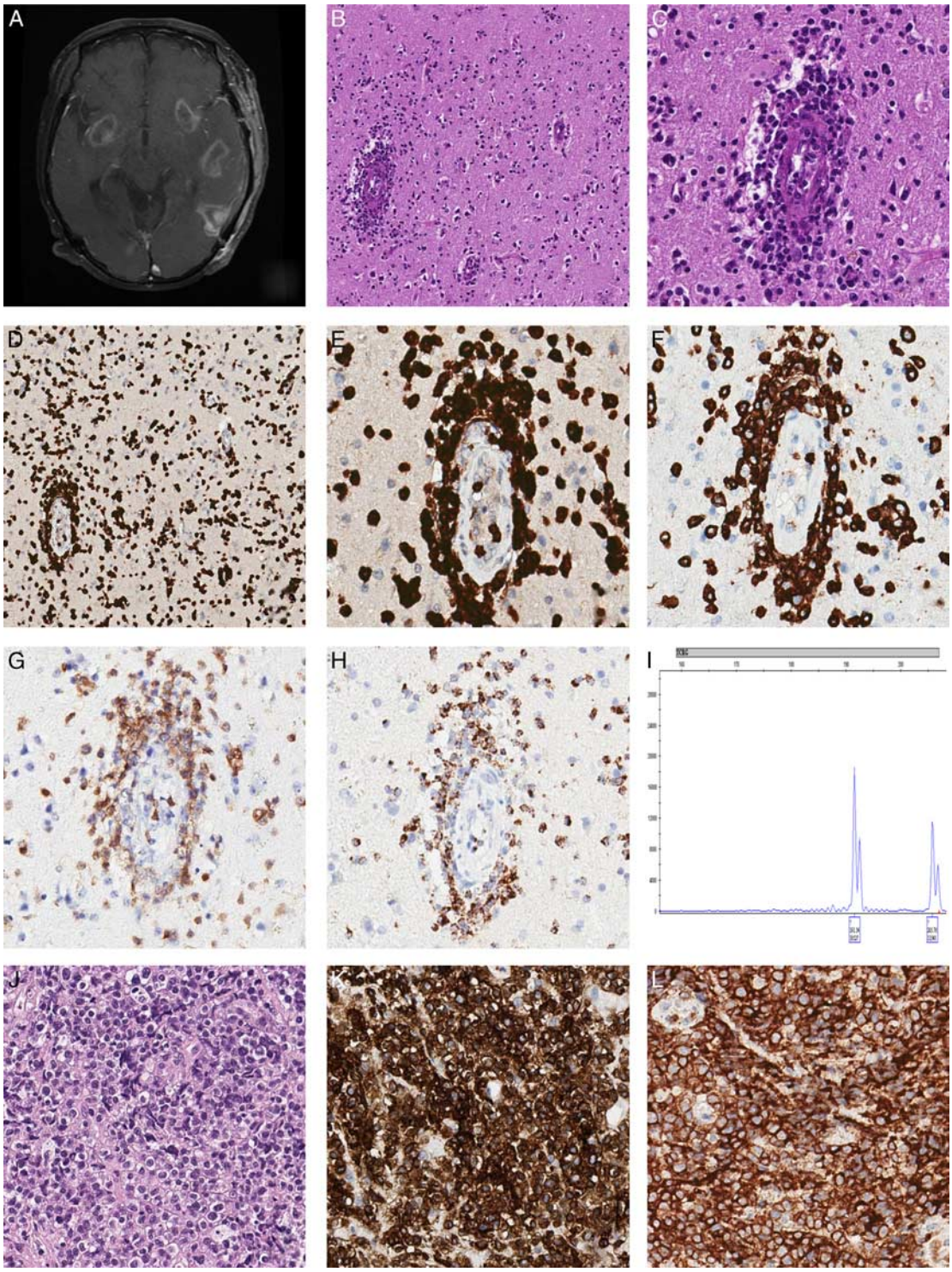

FIGURE 1. Representative images of case 2 (PTCL-NOS) (A–I) and case 9 (PTCL-NOS of γδT-cell lineage) (J–L). In case 2, brain magnetic resonance imaging showed an irregular peripheral enhancing lesion involving the left temporal, parietal, and right occipital lobes (A). Atypical lymphoid cells were infiltrating brain parenchyme with perivascular cuffing (B, C). In immunohistochemistry, tumor cells were positive for CD3 (D, E), CD8 (F), TCRβF1 (G) and granzyme B (H). T-cell monoclonality was observed in a *TCRG* gene rearrangement study (I). Case 9 (PTCL-NOS of γδT-cell origin) showed diffuse infiltration of atypical medium-to-large lymphoid cells (J), which expressed CD3 (K) and TCRγ (L). PTCL-NOS indicates peripheral T-cell lymphoma, not otherwise specified.

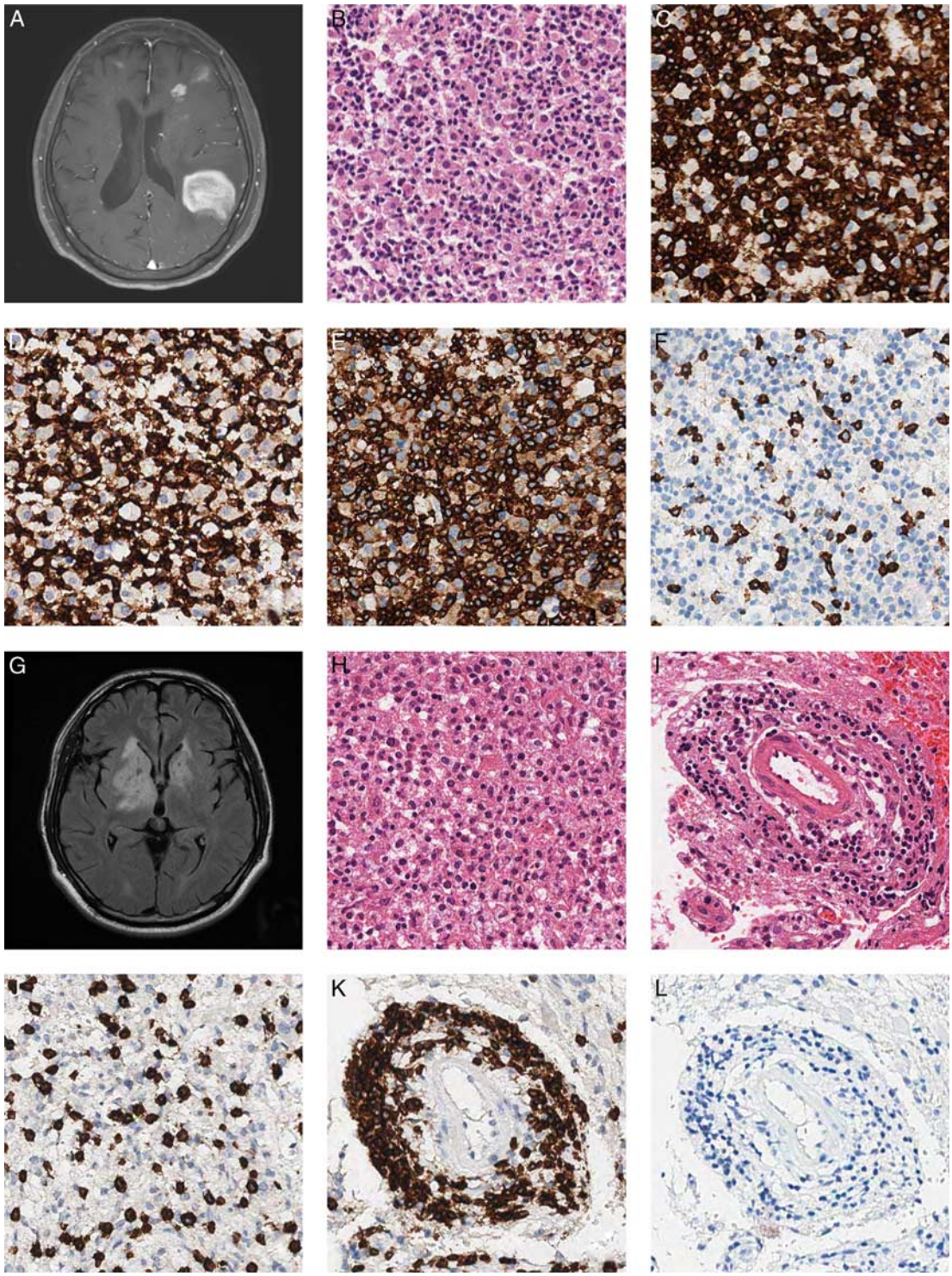

FIGURE 2. Representative images of case 3 (PTCL-NOS) (A–F) and case 8 (PTCL-NOS) (G–L). A, Brain magnetic resonance imaging of case 3 showed multiple enhancing lesions in both cerebral hemispheres (A) and the cerebellum (not shown). Brain parenchyme was diffusely infiltrated by small-to-medium-sized atypical lymphoid cells (B), which expressed CD3 (C), TCRβF1 (D), and CD4 (E). Scattered suspected reactive cells were positive for CD8 (F). G, Brain magnetic resonance imaging of case 8 showed ill-defined T2 high SI lesions in both basal ganglia, the internal capsule, and adjacent white matter. Small-sized lymphoid cells infiltrated brain parenchyme along with perivascular cuffing (H, I). Infiltrating cells were positive for CD3 (J, K) and negative for CD20 (L). PTCL-NOS indicates peripheral T-cell lymphoma, not otherwise specified.

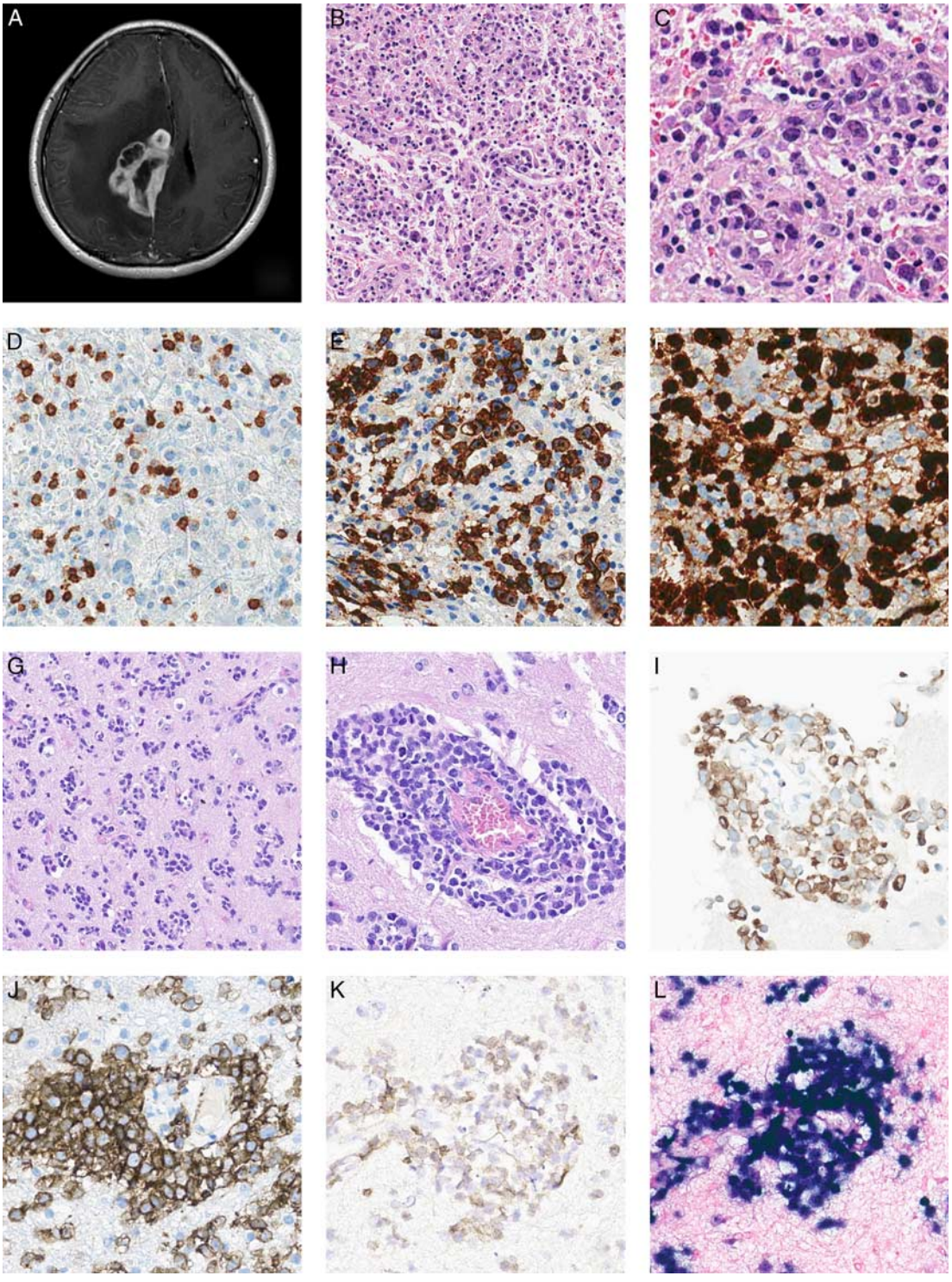

FIGURE 3. Representative images of case 4 (anaplastic lymphoma kinase-positive anaplastic large cell lymphoma) (A–F) and case 11 (extranodal natural killer/T-cell lymphoma of αβT-cell lineage) (G–L). A, Brain magnetic resonance imaging of case 4 showed a solid and cystic mass involving the right cingulate, corpus callosum body and parieto-occipital region. Large pleomorphic anaplastic cells were infiltrating brain parenchyme (B, C). Most of the anaplastic cells were negative for CD3 (D), but positive for CD30 with a strong membranous and Golgi pattern (E), and for anaplastic lymphoma kinase with strong cytoplasmic and nuclear pattern (F). In case 11 (extranodal natural killer/T-cell lymphoma of αβT-cell lineage), large atypical lymphoid cells were infiltrating brain parenchyme along small vasculature or in a perineuronal satellitosis pattern (G). Clear perivascular cuffing of atypical cells was observed (H). Tumor cells were diffusely positive for CD3 (I), CD8 (J), TCRβF1 (K), and Epstein-Barr virus (L).

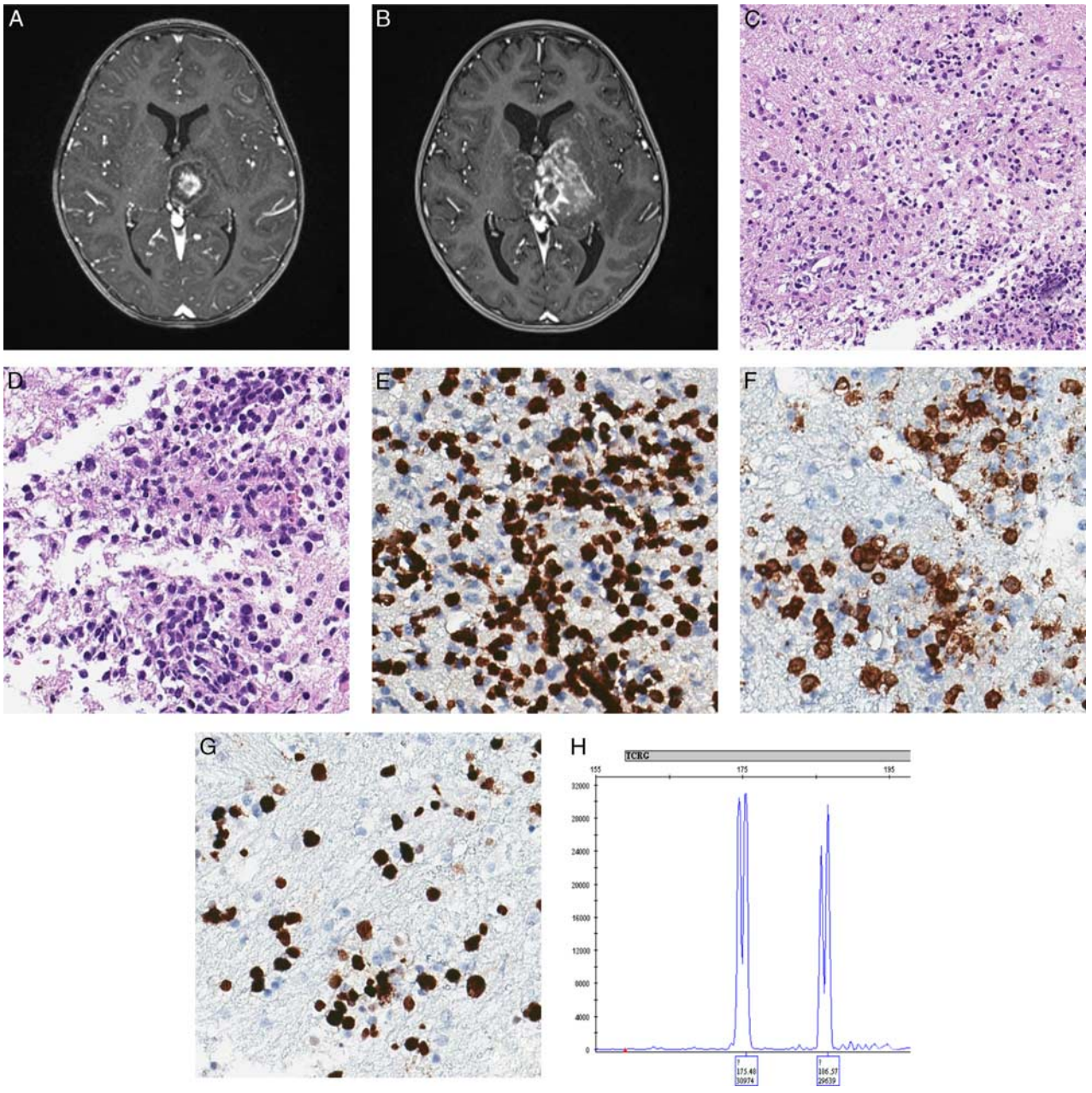

FIGURE 4. Representative images of case 10 (pediatric peripheral T-cell lymphoma, not otherwise specified). A, Initial brain magnetic resonance imaging revealed a 2-cm T2 high SI lesion in the left thalamus. B, One month later, the left thalamic lesion extended into the right thalamus, left basal ganglia, and bilateral brain stem. In biopsy taken after steroid treatment, brain parenchyme was infiltrated by small lymphoid cells (C, D), expressing CD3 (E) and CD8 (F) with Ki-67 (+) proliferative activity (G). H, T-cell monoclonality was observed in a *TCRG* gene rearrangement study.

JAK3. Pathogenic mutations were found in 4 cases. Case 2 had *KMT2C* frameshift mutation (c.1139delG; p.Arg380fs), and case 3 had nonsense mutation in *TET2* (c.1112T > A; p. Leu371*). Case 9 had missense mutations in *NRAS* (c.34G > A; p.Gly12Ser) and *JAK3* (c.1533G > A; p. Met511Ile), and homozygous gene copy deletions in *CDKN2A* (CN = 0) and *CDKN2B* (CN = 0). Case 11 harbored a nonsense mutation in *ARID1B* (c.1274C > A; p. Ser425*), frameshift mutation in *BCOR* (c.472dupA; p. Ser158fs), splicing mutation in *FAS* (c.652-2A > G), and multiple missense mutations in *TP53* (c.404G > T; p. Cys135Phe, c.482C > T; p.Ala161Val, c.524G > A; p. Arg175His). This case also harbored copy number deletions in *KMT2C, POT1*, and *PRDM1*.

DISCUSSION

This study identified the clinical, pathologic, and genetic features of 11 rare cases of T-PCNSL, including 9 of

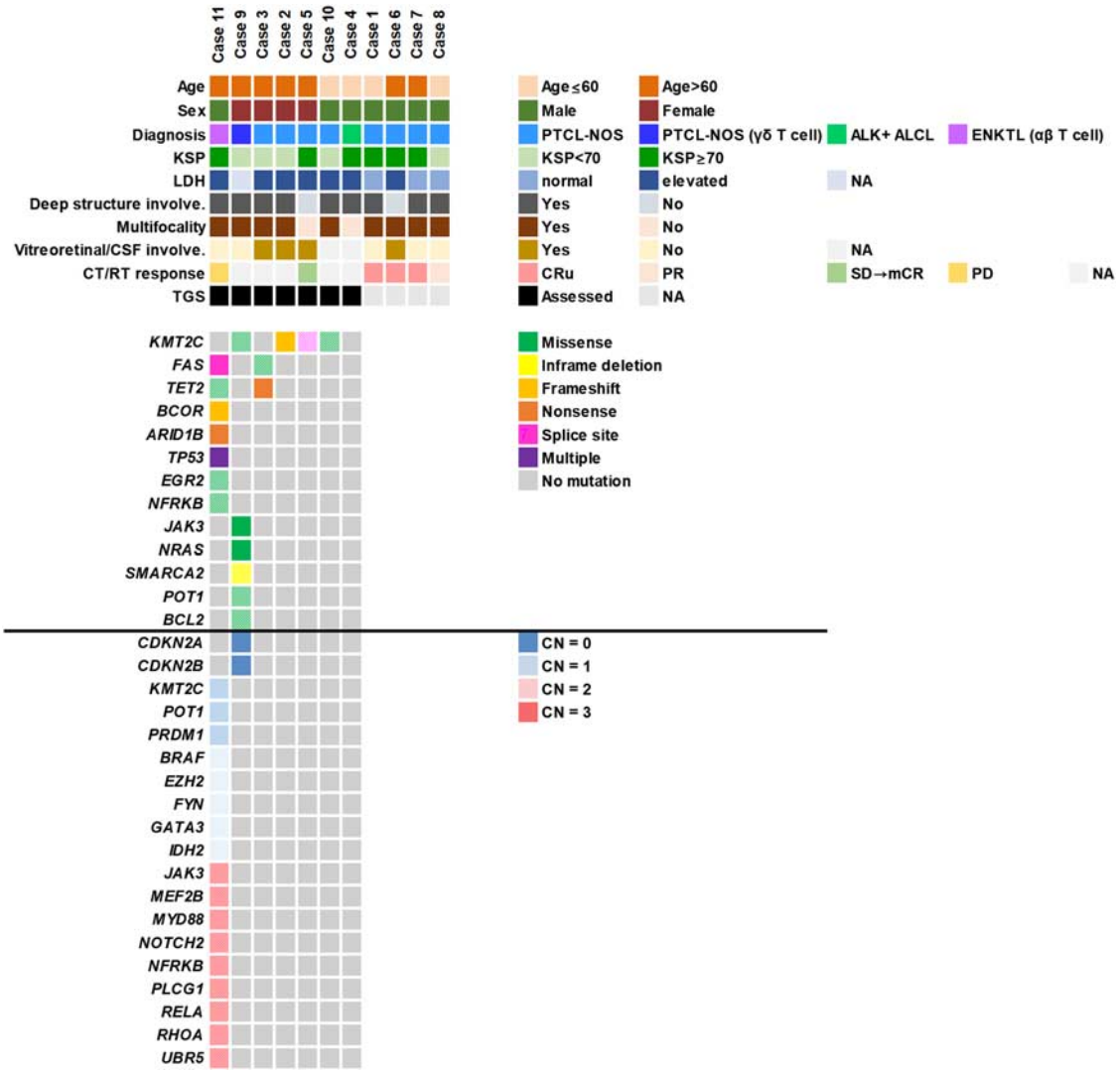

FIGURE 5. Summary of the clinicopathologic characteristics and mutational map of T-primary central nervous system lymphoma. Mutated genes and genes with copy number alteration found by targeted gene sequencing are depicted. Variants of unknown significance are brushed with oblique lines.

PTCL-NOS, 1 of ALK (+) ALCL and 1 of ENKTL. Most of the cases with PTCL-NOS were characterized by small or small-to-medium-sized cells; the cases of PTCL-NOS of γδT-cell lineage and ENKTL were characterized by medium-to-large or large cells. Perivascular lymphocytic infiltration of variable intensity was observed in most cases, similar to PCNS-DLBCL. The majority of cases showed cytotoxic molecule expression, and the proportions of cases with the CD4 and CD8 phenotype were similar. Although our study includes only a limited number of cases, our study reveals that the genetic alterations found in T-PCNSL are similar to that of systemic T-cell lymphomas. The molecular study demonstrated frequent *KMT2C* alterations in T-PCNSL cases, and *NRAS* G12S and *JAK3* M511I mutations, and homozygous deletions of *CDKN2A* and *CDKN2B*, in the case of PTCL with γδT-cell subtype. In one of the cases of PTCL-NOS, truncation mutation of *TET2* was observed. In the case of PCNS-ENKTL, genetic alterations similar to systemic ENKTL were observed.

We confirmed 4 cases (cases 2, 3, 9, and 11) with interesting pathogenic alterations. Case 2 (PTCL-NOS) harbored the frameshift mutation of *KMT2C*. KMT2C (mixed-lineage leukemia 3) is a member of the mixed-lineage leukemia family of histone methyltransferase and methylates histone 3 tail at lysine 4 (H3K4).[10] *KMT2C* was one of the most frequently mutated genes in a targeted sequencing study of PTCL-NOS,[11] with nonsynonymous somatic mutations in 32% (23/71 cases) of samples.

Case 3 (PTCL-NOS) had a nonsense mutation of *TET2*. As *TET2* is an epigenetic regulator and somatic mutations driving aging-associated clonal hematopoiesis readily occur in *TET2*,[12] we additionally performed targeted gene sequencing using the patient's peripheral blood sample. The patient's peripheral blood did not reveal the *TET2* L371* mutation found

in the patient's brain lesion, confirming that it is a mutation of the tumor rather than clonal hematopoiesis. *TET2* mutations were identified in PTCL (64/190 cases), including angioimmunoblastic T-cell lymphoma (40/86 cases), PTCL-NOS (22/58 cases), and enteropathy-associated T-cell lymphoma (EATL) (2/10 cases).[13] In particular, *TET2* mutations were observed at a higher frequency (14/24, 58%) in PTCL-NOS cases positive for T_{FH} markers.[13] *TET2* mutation was reported in 1 (T-PCNSL of γδT-cell type) of the 11 patients with T-PCNSL reported by Menon et al,[7] and 1 of the 6 patients with T-PCNSL in this study harbored a pathogenic *TET2* mutation. This suggests that *TET2* also plays a key role in the pathogenesis of T-cell lymphoma arising in the CNS.

The case of PTCL of γδT-cell lineage (case 9) was especially intriguing. Missense mutations of *NRAS* (c.34G > A; p.Gly12Ser) and *JAK3* (c.1533G > A; p.Met511Ile), as well as homozygous deletions of *CDKN2A* and *CDKN2B*, were found. *NRAS*, a GTPase, is mutated in a diverse range of hematolymphoid and non-hematolymphoid cancers.[14–23] Codons 12, 13, and 61 of *NRAS* are well-known hotspots of multiple oncogenic mutations,[24] and are prognostic predictors for targeted therapy.[25] Activating mutations of the Janus kinase (JAK)/signal transducer and activator of transcription (STAT) pathway have been reported in hepatosplenic γδT-cell lymphoma (HSTL)[26,27] and non-HSTL, including cutaneous γδT-cell lymphomas and type II EATL (currently monomorphic epitheliotropic intestinal T-cell lymphoma),[28,29] as well as in other peripheral T-cell lymphomas including ALCL,[30,31] adult T-cell leukemia/lymphoma (ATLL),[32] ENKTL,[33,34] large granular lymphocytic leukemia,[35,36] and T-cell prolymphocytic leukemia (T-PLL).[37] In particular, *JAK3* M511I mutation has been described in type II EATL,[38] T-ALL,[39,40] T-PLL,[41] and AML.[42] Menon et al found *JAK3* M511I mutations in 1 case with PTCL-NOS (αβT-cell phenotype) among 11 T-PCNSL cases.[7] Also considering our case, *JAK3* M511I mutation appears to be a recurrent mutation in T-PCNSL and a potential therapeutic target.[29] Among T-cell lymphomas, *CDKN2A–CDKN2B* locus inactivation has been reported in cutaneous T-cell lymphomas (CTCLs) and *CDKN2A–CDKN2B* deletion was more specific to an aggressive subset of CTCL.[43] Notably, case 9 had the worst prognosis among this study cohort; she initially presented with extensive disease and died within 3 months of diagnosis. This dismal outcome could be partly explained by the relatively high mutational burden, where there were also perturbations in the RAS pathway, JAK/STAT pathway, and cell cycle regulatory pathway. Furthermore, a hotspot mutation of *JAK3* was found in a previous series and our study, suggesting the potential role of this alteration in the T-cell lymphomagenesis within the CNS.

Primary CNS ENKTL is an extremely rare entity; to the best of our knowledge, only 14 cases have been reported in the literature[44–50] and the molecular characteristics of primary CNS ENKTL have not been elucidated. Our primary CNS ENKTL case (case 11) showed multiple genetic mutations, including *ARID1B* (c.1274C > A; p.Ser425*), *BCOR* (c.472dupA; p.Ser158fs), *FAS* (c.652-2A > G; splicing), and *TP53* (c.404G > T; p.Cys135Phe, c.482C > T; p.Ala161Val, c.524G > A; p.Arg175His), as well as heterozygous deletions in *KMT2C, POT1*, and *PRDM1*. *BCOR* (BCL-6 interacting corepressor) is one of the most frequently mutated genes in ENKTL (21% to 32% of cases) and suspected to play a tumor suppressive or oncogenic role depending on the mutation type.[51,52] Loss-of-function mutations of *BCOR* have been reported in 32% of ENKTL cases, suggesting that *BCOR* acts as an important tumor suppressor in lymphomagenesis.[51] Mutations of FAS (CD95/Apo-1, a well-known death receptor) may result in resistance to apoptosis and tumor immune privilege, and was recurrently reported in ENKTL.[53,54] The *TP53* gene is one of the top three genes mutated in ENKTL (up to 63% of cases).[55] *PRDM1* (encoding Blimp1, a zinc-finger motif-containing transcriptional repressor) plays a regulatory role in the homeostasis of T cells and NK cells.[56] *PRDM1* and its loci, the 6q21-6q25 region, was frequently deleted in ENKTL and other NK cell malignancies.[57,58] In non-CNS ENKTL, genetic alterations in KMT2C were found in 16% of cases.[59] Taken together, these findings suggested that PCNS-NKTL might be classifiable as non-CNS ENKTL, as it shares common pathogenic gene alterations.

In conclusion, this study showed that T-PCNSL is a heterogeneous entity with various clinical and morphologic presentations. Mutations in a subset of genes, which were reported to be significant in the pathogenesis of T-cell lymphoma in other organs, were also found in this series, and we showed that multiple perturbations on key pathways were associated with a dismal outcome, albeit only in 1 case. Further studies in a larger study population should lead to a better understanding of this rare disease.

REFERENCES

1. Swerdlow S, Campo E, Harris N. *WHO Classification of Tumours of Haemotopoietic and Lymphoid Tissues*. Lyon: International Agency for Research on Cancer; 2017.
2. Ferreri AJ, Reni M, Pasini F, et al. A multicenter study of treatment of primary CNS lymphoma. *Neurology*. 2002;58:1513–1520.
3. Bataille B, Delwail V, Menet E, et al. Primary intracerebral malignant lymphoma: report of 248 cases. *J Neurosurg*. 2000;92:261–266.
4. Hayabuchi N, Shibamoto Y, Onizuka Y. Primary central nervous system lymphoma in Japan: a nationwide survey. *Int J Radiat Oncol Biol Phys*. 1999;44:265–272.
5. Lim T, Kim SJ, Kim K, et al. Primary CNS lymphoma other than DLBCL: a descriptive analysis of clinical features and treatment outcomes. *Ann Hematol*. 2011;90:1391–1398.
6. Shenkier TN, Blay JY, O'Neill BP, et al. Primary CNS lymphoma of T-cell origin: a descriptive analysis from the international primary CNS lymphoma collaborative group. *J Clin Oncol*. 2005;23:2233–2239.
7. Menon MP, Nicolae A, Meeker H, et al. Primary CNS T-cell lymphomas: a clinical, morphologic, immunophenotypic, and molecular analysis. *Am J Surg Pathol*. 2015;39:1719–1729.
8. Yim J, Song SG, Kim S, et al. Primary peripheral gamma delta T-cell lymphoma of the central nervous system: report of a case involving the intramedullary spinal cord and presenting with myelopathy. *J Pathol Transl Med*. 2019;53:57–61.
9. Signoretti S, Murphy M, Cangi MG, et al. Detection of clonal T-cell receptor gamma gene rearrangements in paraffin-embedded tissue by polymerase chain reaction and nonradioactive single-strand conformational polymorphism analysis. *Am J Pathol*. 1999;154:67–75.
10. Rampias T, Karagiannis D, Avgeris M, et al. The lysine-specific methyltransferase KMT2C/MLL3 regulates DNA repair components in cancer. *EMBO Rep*. 2019;20:e46821.
11. Laginestra MA, Cascione L, Motta G, et al. Whole exome sequencing reveals mutations in FAT1 tumor suppressor gene clinically impacting on peripheral T-cell lymphoma not otherwise specified. *Mod Pathol*. 2020;33:179–187.

12. Buscarlet M, Provost S, Zada YF, et al. DNMT3A and TET2 dominate clonal hematopoiesis and demonstrate benign phenotypes and different genetic predispositions. *Blood*. 2017;130:753–762.
13. Lemonnier F, Couronne L, Parrens M, et al. Recurrent TET2 mutations in peripheral T-cell lymphomas correlate with TFH-like features and adverse clinical parameters. *Blood*. 2012;120:1466–1469.
14. Jakob JA, Bassett RL Jr, Ng CS, et al. NRAS mutation status is an independent prognostic factor in metastatic melanoma. *Cancer*. 2012;118:4014–4023.
15. Fakhruddin N, Jabbour M, Novy M, et al. BRAF and NRAS mutations in papillary thyroid carcinoma and concordance in BRAF mutations between primary and corresponding lymph node metastases. *Sci Rep*. 2017;7:4666.
16. Tyner JW, Tognon CE, Bottomly D, et al. Functional genomic landscape of acute myeloid leukaemia. *Nature*. 2018;562:526–531.
17. Wang S, Wu Z, Li T, et al. Mutational spectrum and prognosis in NRAS-mutated acute myeloid leukemia. *Sci Rep*. 2020;10:12152.
18. Carr RM, Vorobyev D, Lasho T, et al. RAS mutations drive proliferative chronic myelomonocytic leukemia via a KMT2A-PLK1 axis. *Nat Commun*. 2021;12:2901.
19. Liang DC, Chen SH, Liu HC, et al. Mutational status of NRAS, KRAS, and PTPN11 genes is associated with genetic/cytogenetic features in children with B-precursor acute lymphoblastic leukemia. *Pediatr Blood Cancer*. 2018;65:e26786.
20. Vendramini E, Bomben R, Pozzo F, et al. KRAS, NRAS, and BRAF mutations are highly enriched in trisomy 12 chronic lymphocytic leukemia and are associated with shorter treatment-free survival. *Leukemia*. 2019;33:2111–2115.
21. Walker BA, Boyle EM, Wardell CP, et al. Mutational spectrum, copy number changes, and outcome: results of a sequencing study of patients with newly diagnosed myeloma. *J Clin Oncol*. 2015;33:3911–3920.
22. Pasca S, Tomuleasa C, Teodorescu P, et al. KRAS/NRAS/BRAF mutations as potential targets in multiple myeloma. *Front Oncol*. 2019;9:1137.
23. Diamond EL, Durham BH, Ulaner GA, et al. Efficacy of MEK inhibition in patients with histiocytic neoplasms. *Nature*. 2019;567:521–524.
24. Hobbs GA, Der CJ, Rossman KL. RAS isoforms and mutations in cancer at a glance. *J Cell Sci*. 2016;129:1287–1292.
25. Dummer R, Schadendorf D, Ascierto PA, et al. Binimetinib versus dacarbazine in patients with advanced NRAS-mutant melanoma (NEMO): a multicentre, open-label, randomised, phase 3 trial. *Lancet Oncol*. 2017;18:435–445.
26. Nicolae A, Xi L, Pittaluga S, et al. Frequent STAT5B mutations in gammadelta hepatosplenic T-cell lymphomas. *Leukemia*. 2014;28:2244–2248.
27. McKinney M, Moffitt AB, Gaulard P, et al. The genetic basis of hepatosplenic T-cell lymphoma. *Cancer Discov*. 2017;7:369–379.
28. Kucuk C, Jiang B, Hu X, et al. Activating mutations of STAT5B and STAT3 in lymphomas derived from gammadelta-T or NK cells. *Nat Commun*. 2015;6:6025.
29. Nairismagi ML, Tan J, Lim JQ, et al. JAK-STAT and G-protein-coupled receptor signaling pathways are frequently altered in epitheliotropic intestinal T-cell lymphoma. *Leukemia*. 2016;30:1311–1319.
30. Anastasov N, Bonzheim I, Rudelius M, et al. C/EBPbeta expression in ALK-positive anaplastic large cell lymphomas is required for cell proliferation and is induced by the STAT3 signaling pathway. *Haematologica*. 2010;95:760–767.
31. Crescenzo R, Abate F, Lasorsa E, et al. Convergent mutations and kinase fusions lead to oncogenic STAT3 activation in anaplastic large cell lymphoma. *Cancer Cell*. 2015;27:516–532.
32. Kataoka K, Nagata Y, Kitanaka A, et al. Integrated molecular analysis of adult T cell leukemia/lymphoma. *Nat Genet*. 2015;47:1304–1315.
33. Koo GC, Tan SY, Tang T, et al. Janus kinase 3-activating mutations identified in natural killer/T-cell lymphoma. *Cancer Discov*. 2012;2:591–597.
34. Bouchekioua A, Scourzic L, de Wever O, et al. JAK3 deregulation by activating mutations confers invasive growth advantage in extranodal nasal-type natural killer cell lymphoma. *Leukemia*. 2014;28:338–348.
35. Koskela HL, Eldfors S, Ellonen P, et al. Somatic STAT3 mutations in large granular lymphocytic leukemia. *N Engl J Med*. 2012;366:1905–1913.
36. Jerez A, Clemente MJ, Makishima H, et al. STAT3 mutations unify the pathogenesis of chronic lymphoproliferative disorders of NK cells and T-cell large granular lymphocyte leukemia. *Blood*. 2012;120:3048–3057.
37. Kiel MJ, Velusamy T, Rolland D, et al. Integrated genomic sequencing reveals mutational landscape of T-cell prolymphocytic leukemia. *Blood*. 2014;124:1460–1472.
38. Roberti A, Dobay MP, Bisig B, et al. Type II enteropathy-associated T-cell lymphoma features a unique genomic profile with highly recurrent SETD2 alterations. *Nat Commun*. 2016;7:12602.
39. Zhang J, Ding L, Holmfeldt L, et al. The genetic basis of early T-cell precursor acute lymphoblastic leukaemia. *Nature*. 2012;481:157–163.
40. Vicente C, Schwab C, Broux M, et al. Targeted sequencing identifies associations between IL7R-JAK mutations and epigenetic modulators in T-cell acute lymphoblastic leukemia. *Haematologica*. 2015;100:1301–1310.
41. Bergmann AK, Schneppenheim S, Seifert M, et al. Recurrent mutation of JAK3 in T-cell prolymphocytic leukemia. *Genes Chromosomes Cancer*. 2014;53:309–316.
42. Yamashita Y, Yuan J, Suetake I, et al. Array-based genomic resequencing of human leukemia. *Oncogene*. 2010;29:3723–3731.
43. Laharanne E, Chevret E, Idrissi Y, et al. CDKN2A-CDKN2B deletion defines an aggressive subset of cutaneous T-cell lymphoma. *Mod Pathol*. 2010;23:547–558.
44. Miyata-Takata T, Takata K, Kato S, et al. Clinicopathological analysis of primary central nervous system NK/T cell lymphoma: rare and localized aggressive tumour among extranasal NK/T cell tumours. *Histopathology*. 2017;71:287–295.
45. Ng SB, Lai KW, Murugaya S, et al. Nasal-type extranodal natural killer/T-cell lymphomas: a clinicopathologic and genotypic study of 42 cases in Singapore. *Mod Pathol*. 2004;17:1097–1107.
46. Kaluza V, Rao DS, Said JW, et al. Primary extranodal nasal-type natural killer/T-cell lymphoma of the brain: a case report. *Hum Pathol*. 2006;37:769–772.
47. Guan H, Huang Y, Wen W, et al. Primary central nervous system extranodal NK/T-cell lymphoma, nasal type: case report and review of the literature. *J Neurooncol*. 2011;103:387–391.
48. Prajapati HJ, Vincentelli C, Hwang SN, et al. Primary CNS natural killer/T-cell lymphoma of the nasal type presenting in a woman: case report and review of the literature. *J Clin Oncol*. 2014;32:e26–e29.
49. Liao B, Kamiya-Matsuoka C, Gong Y, et al. Primary natural killer/T-cell lymphoma presenting as leptomeningeal disease. *J Neurol Sci*. 2014;343:46–50.
50. Li LF, Taw BB, Pu JK, et al. Primary central nervous system natural killer cell lymphoma in a chinese woman with atypical (11)C-choline positron emission tomography and magnetic resonance spectrometry findings. *World Neurosurg*. 2015;84:1176.e1175–1176.e1179.
51. Dobashi A, Tsuyama N, Asaka R, et al. Frequent BCOR aberrations in extranodal NK/T-Cell lymphoma, nasal type. *Genes Chromosomes Cancer*. 2016;55:460–471.
52. Lee S, Park HY, Kang SY, et al. Genetic alterations of JAK/STAT cascade and histone modification in extranodal NK/T-cell lymphoma nasal type. *Oncotarget*. 2015;6:17764–17776.
53. Takakuwa T, Dong Z, Nakatsuka S, et al. Frequent mutations of Fas gene in nasal NK/T cell lymphoma. *Oncogene*. 2002;21:4702–4705.
54. Shen L, Liang AC, Lu L, et al. Frequent deletion of Fas gene sequences encoding death and transmembrane domains in nasal natural killer/T-cell lymphoma. *Am J Pathol*. 2002;161:2123–2131.
55. Zhang Y, Li C, Xue W, et al. Frequent mutations in natural killer/T cell lymphoma. *Cell Physiol Biochem*. 2018;49:1–16.
56. de Mel S, Hue SS, Jeyasekharan AD, et al. Molecular pathogenic pathways in extranodal NK/T cell lymphoma. *J Hematol Oncol*. 2019;12:33.
57. Iqbal J, Kucuk C, Deleeuw RJ, et al. Genomic analyses reveal global functional alterations that promote tumor growth and novel tumor suppressor genes in natural killer-cell malignancies. *Leukemia*. 2009;23:1139–1151.
58. Kucuk C, Iqbal J, Hu X, et al. PRDM1 is a tumor suppressor gene in natural killer cell malignancies. *Proc Natl Acad Sci U S A*. 2011;108:20119–20124.
59. Xiong J, Cui BW, Wang N, et al. Genomic and transcriptomic characterization of natural killer T cell lymphoma. *Cancer Cell*. 2020;37:403–419.e406.

